Dwarfs and Giants: Cannibalism and Competition in Size-Structured Populations

David Claessen,[1,*] André M. de Roos,[1,†] and Lennart Persson[2,‡]

1. Population Biology Section, University of Amsterdam, Kruislaan 320, 1098 SM Amsterdam, The Netherlands;
2. Department of Ecology and Environmental Science, Aquatic Ecology Group, Umeå University, S-901 87 Umeå, Sweden

ABSTRACT: Cannibals and their victims often share common resources and thus potentially compete. Smaller individuals are often competitively superior to larger ones because of size-dependent scaling of foraging and metabolic rates, while larger ones may use cannibalism to counter this competition. We study the interplay between cannibalism and competition using a size-structured population model in which all individuals consume a shared resource but in which larger ones may cannibalize smaller conspecifics. In this model, intercohort competition causes single-cohort cycles when cannibalism is absent. Moderate levels of cannibalism reduce intercohort competition, enabling coexistence of many cohorts. More voracious cannibalism, in combination with competition, produces large-amplitude cycles and a bimodal population size distribution with many small and few giant individuals. These coexisting "dwarfs" and "giants" have very different life histories, resulting from a reversal in importance of cannibalism and competition. The population structure at time of birth determines whether individuals suffer severe cannibalism, with the few survivors reaching giant sizes, or whether they suffer intense intracohort competition, with all individuals remaining small. These model results agree remarkably well with empirical data on perch population dynamics. We argue that the induction of cannibalistic giants in piscivorous fish is a population-dynamic emergent phenomenon that requires a combination of size-dependent cannibalism and competition.

Keywords: size-dependent cannibalism, competition, structured-population model, "double" growth curves, *Perca fluviatilis*.

* To whom correspondence should be addressed; e-mail: claessen@bio.uva.nl.

† E-mail: aroos@bio.uva.nl.

‡ E-mail: lennart.persson@eg.umu.se.

Cannibalism is widespread in the animal kingdom and is particularly common in arthropods, fish, and amphibians (Fox 1975; Polis 1981; Elgar and Crespi 1992). Theoretical studies have shown a diversity of potential effects of cannibalism on population dynamics. Cannibalism may save a population from extinction, a phenomenon referred to as the "lifeboat mechanism" (Van den Bosch et al. 1988; Henson 1997), or may even lead to multiple stable states (Botsford 1981; Fisher 1987; Cushing 1991, 1992). Recent experimental and model studies of the flour beetle *Tribolium* show that egg cannibalism may induce complex dynamics, including chaos (Costantino et al. 1997; Benoît et al. 1998), which confirms the earlier hypothesis that it may induce population fluctuations (Fox 1975; Diekmann et al. 1986; Hastings 1987). Conversely, cannibalism can dampen fluctuations, for example, in population models that exhibit age-dependent, single-generation cycles (Van den Bosch and Gabriel 1997).

Physiological and behavioral constraints, such as gape size limitation and mobility, make cannibalism inherently size dependent. Generally, a cannibal is considerably larger than its victim (Fox 1975; Polis 1981; Elgar and Crespi 1992; Persson et al. 2000). This size difference between cannibals and their victims also implies a potential for size-dependent competition (Persson et al. 1998). Empirical studies suggest that cannibals and their victims often compete for shared resources (Persson 1988; Polis 1988; Anholt 1994; Fincke 1994). Overlapping diets of cannibals and victims are observed in many taxa (Fox 1975; Polis 1981), notably amphibians (Simon 1984) and fish (Dominey and Blumer 1984). Yet previous studies of the effect of cannibalism on population dynamics have rarely taken the competitive interaction into account (Dong and DeAngelis 1998). Studies of structured population models have shown that size-dependent competition is likely to generate cycles. Smaller individuals are often competitively superior to larger ones because metabolic requirements increase faster with body size than foraging capacity. In systems with pulsed reproduction, such competitive asymmetry may result in single-cohort cycles in which every new generation outcompetes the previous one (Persson et

al. 1998). Single-cohort cycles are analogous to the single-generation cycles that may be found when reproduction is continuous (Gurney and Nisbet 1985).

Cannibalism gives larger individuals the opportunity to reduce competition by smaller ones, for it reduces the density of competitors. In addition, the energy gain from cannibalism reduces the sensitivity of cannibals to competition for other resources. When the energy gain is sufficient to cover energetic needs, cannibals may escape competition altogether. The effect of size-dependent cannibalism on population dynamics may thus counteract the effect of size-dependent competition. Competition and cannibalism may also interfere via their effect on individual growth rates. Competition reduces the growth rate (Alm 1952; Botsford 1981; Post et al. 1999) and impedes an individual in reaching a size sufficiently large to shift to cannibalism. High cannibalistic mortality within a cohort of juveniles reduces intracohort competition and thus increases their growth rate, enabling the survivors to switch to cannibalism. Hence, the timing of the ontogenetic niche shift from, for example, planktivory to piscivory in fish may be the result of the dynamic interplay between size-dependent competition and cannibalism. Also, the growth rate of a cannibal may be much larger than that of noncannibalistic conspecifics, resulting in phenotypic differences, referred to as "cannibalistic polyphenism" (Bragg 1965; Polis 1981).

The focus of this article is the population-dynamic consequences of the mixture of size-dependent cannibalistic and competitive interactions. We formulate a physiologically structured population model of a cannibalistic consumer population with one alternative, unstructured food resource. At the individual level, this model describes the "vital rates" of the organism, that is, growth, consumption, metabolic, and mortality rates as functions of the state of the individual and its environment. Cannibalism is incorporated as an interaction of which the outcome depends on the lengths of two encountering individuals. The impact of cannibalism is studied by varying a parameter that can be interpreted as proportional to the cannibalistic voracity. We find qualitatively different population-dynamic patterns and individual life histories for different ranges of cannibalistic voracity. To study the mechanisms that cause these patterns, the dynamics of both the total abundance and the size structure of the cannibalistic population are analyzed.

The results of our model analysis are confronted with data on time series and individual growth trajectories from a population of Eurasian perch (*Perca fluviatilis*) in a forest lake in central Sweden. Perch is the only fish species in this lake, and perch are known to shift to piscivory, and hence to cannibalism, at larger body sizes (Alm 1952; Persson 1988; Le Cren 1992; Christensen 1997). We argue that

the observed population dynamics and the emergence of a few giant individuals with "double" growth curves (sensu Le Cren 1992) are the result of the dynamic interplay between cannibalism and competition.

The Model

We model the cannibalistic consumer population using a physiologically structured population model that describes the population dynamics explicitly in terms of individual-level processes like growth, reproduction, and mortality (Metz and Diekmann 1986; De Roos et al. 1992; De Roos 1997). Within this framework, a clear distinction is made between state variables at the individual and population level, often referred to as the "*i*-state" and the "*p*-state" variables, respectively. At the individual level, our model describes how individuals may interact with each other and with the resource population, dependent on their physiological state (*i*-state). The population state is given by the distribution of individuals over all possible individual states. The alternative resource is modeled as an unstructured population. What interactions actually occur at a given time depends on both the individual state, the population state, and the resource density.

The Individual-Level Model

Our model is an extension of the consumer-resource model described by Persson et al. (1998). Apart from the cannibalistic interaction, a full substantiation of our model can be found in their article. Here we present a brief outline of our model and its biological assumptions. The cannibalistic interaction among individuals is a unique extension, and therefore we discuss it in more detail. The model equations are given in table 1.

The model parameters are presented in table 2 and are valid for Eurasian perch (*Perca fluviatilis*) with size-dependent cannibalism and competition for a zooplankton resource. We assume that a growing season lasts 90 d, as it does in central Sweden. We assume that biological activity is negligible outside the growing season and take the state of the system at the start of a growing season ("spring") to be identical to that at the end of the previous one.

The feeding, growth, reproduction, and mortality of an individual are assumed to be functions of its body mass. In order to account for starvation and fecundity, we distinguish between irreversible and reversible mass as independent *i*-state variables, referred to as x and y, respectively. Irreversible mass is structural mass, such as bones and vital organs, that cannot be starved away, as opposed to reversible mass (i.e., the reserves). We assume that perch can starve away gonad tissue, which hence is

Table 1: The model equations by subject

Subject	Model equation
Standardized weight	$w = x(1 + q_j)$
Length	$\ell = \lambda_1 w^{\lambda_2}$
Zooplankton attack rate	$A_z(w) = \hat{A}\left[\dfrac{w}{w_{opt}}\exp\left(1 - \dfrac{w}{w_{opt}}\right)\right]^{\alpha}$
Cannibalistic attack rate	$A_c(c, v) = \begin{cases} \beta c^{\sigma}\dfrac{v - \delta c}{(\varphi - \delta)c} & \text{if } \delta c < v \leq \varphi c \\[2ex] \beta c^{\sigma}\dfrac{\varepsilon c - v}{(\varepsilon - \varphi)c} & \text{if } \varphi c < v < \varepsilon c \\[2ex] 0 & \text{otherwise} \end{cases}$
Food intake rate	$I(x_i) = \dfrac{\eta(x_i)}{1 + H(w_i)\eta(x_i)}$
Handling time	$H(w_i) = \xi_1 w_i^{\xi_2}$
Total encounter rate	$\eta(x_i) = \eta_z(x_i) + \eta_c(x_i)$
Zooplankton encounter	$\eta_z(x_i) = A_z(w_i)Rm$
Cannibalistic encounter	$\eta_c(x_i) = \sum_j A_c(c_i, v_j)(x_j + y_j)N_j$
Energy balance	$E_g(x, y) = E_a(x) - E_m(x, y)$
Acquired energy	$E_a(x) = k_e I(x)$
Maintenance requirements	$E_m(x, y) = \rho_1(x + y)^{\rho_2}$
Fecundity	$F(x, y) = \begin{cases} k_r(y - q_j x)/w_b & \text{if } x > x_f \text{ and } y > q_j x \\ 0 & \text{otherwise} \end{cases}$
Total mortality	$\mu(x, y) = \mu_0 + \mu_s(x, y) + \mu_c(x)$
Starvation mortality	$\mu_s(x, y) = \begin{cases} s(q_s x/y - 1) & \text{if } y < q_s x \\ 0 & \text{otherwise} \end{cases}$
Cannibalistic mortality	$\mu_c(x_j) = \sum_i \dfrac{A_c(c_i, v_j)N_i}{1 + H(w_i)\eta(x_i)}$
Resource dynamics	$\dfrac{dR}{dt} = r(K - R) - R\sum_i \dfrac{A_z(w_i)N_i}{1 + H(w_i)\eta(x_i)}$

Note: Equations and symbols are explained in the text. Only the subscripts i and j refer to the cohort index.

Table 2: Model variables and parameters valid for Eurasian perch (*Perca fluviatilis*) feeding on a zooplankton resource[a] and conspecifics

Subject and symbol	Value	Unit	Interpretation	Reference
i-state variables:				
x	…	g	Irreversible mass	…
y	…	g	Reversible mass	…
Season:				
Y	90	d	Length of year	…
Ontogeny:				
w_b	1.8E−03	g	Egg size (total weight)	Byström and Garcia-Berthóu 1999; P. Byström, unpublished data
x_f	4.6	g	Maturation bone mass	Byström and Garcia-Berthóu 1999; P. Byström, unpublished data
q_J	.74	…	Juvenile maximum condition	Treasurer 1981
q_A	1.37	…	Adult maximum condition	L. Persson, unpublished data
k_r	.5	…	Gonad-offspring conversion	
Length-weight:				
λ_1	48.3	mm g$^{-\lambda_2}$	Allometric scalar	Byström and Garcia-Berthóu 1999; P. Byström, unpublished data
λ_2	.317	…	Allometric exponent	Byström and Garcia-Berthóu 1999; P. Byström, unpublished data
Planktivory:				
α	.62	…	Allometric exponent	Byström and Garcia-Berthóu 1999; P. Byström, unpublished data
$\hat{A}$	3.0E+04	L/d	Maximum attack rate	Persson 1987
w_{opt}	8.2	g	Optimal forager size	Persson and Greenberg 1990
Piscivory:				
σ	.6	…	Allometric exponent	B. Christensen, unpublished data
β	Varied	L d^{-1} mm$^\alpha$	Cannibalistic voracity	B. Christensen, unpublished data
δ	.06	m/m	Minimum victim/cannibal	Popova and Sytina 1977; Willemsen 1977; Buijse and Van Densen 1992; Eklöv and Diehl 1994; Van Densen 1994; Christensen 1996; Lundvall et al. 1999; Persson et al. 2000
ε	.45	m/m	Maximum victim/cannibal	Popova and Sytina 1977; Willemsen 1977; Buijse 1992; Eklöv and Diehl 1994; Van Densen 1994; Christensen 1996; Lundvall et al. 1999; Persson et al. 2000
φ	.2	m/m	Optimal victim/cannibal	Lundvall et al. 1999
Handling:				
ξ_1	5.0	d g$^{-(1+\xi_2)}$	Allometric scalar	Lessmark 1983; P. Byström, unpublished data
ξ_2	−.8	…	Allometric exponent	Lessmark 1983; P. Byström, unpublished data
Metabolism:				
ρ_1	.033	g$^{(1-\rho_2)}$ d^{-1}	Allometric scalar	Beamish 1974; Elliott 1976; Kitchell et al. 1977; Karås and Thoresson 1992
ρ_2	.77	…	Allometric exponent	Beamish 1974; Elliott 1976; Kitchell et al. 1977; Karås and Thoresson 1992
k_e	.61	…	Intake coefficient	Solomon and Brafield 1972; Beamish 1974; Elliott 1976; Rice et al. 1983; Karås and Thoresson 1992
Mortality:				
μ_0	.01	d^{-1}	Background rate	Byström and Garcia-Berthóu 1999; P. Byström, unpublished data; B. Christensen, unpublished data
q_s	.2	…	Starvation condition	…
s	.2	d^{-1}	Starvation coefficient	…
Resource:				
R	…	L^{-1}	Resource population density	…
r	.1	d^{-1}	Population growth rate	…
K	100.0	L^{-1}	Carrying capacity	L. Persson, unpublished data; E. Wahlström, unpublished data
m	3.0E−5	g	Wet weight 1.0 mm *Daphnia*	Byström and Garcia-Berthóu 1999; P. Byström unpublished data

Note: All parameters except Y, r, and K refer to individual level processes.

[a] *Daphnia* sp., length 1 mm.

part of the reversible mass. We assume that the ratio y/x is a measure of the condition of an individual. Total body length, zooplankton attack rate, cannibalistic attack rate, and gut volume are assumed to depend on irreversible mass only. In the following, weight and mass refer to wet weight. In principle, modeling and parameterization of consumption and digestion of prey tissue require conversions between volume, energy content, and dry or wet weight of the prey. To keep things simple, however, we always refer to wet weight.

An important part of the individual-level model concerns the channeling of acquired energy. We assume that maintenance is covered first, such that net energy production (E_g) equals the difference between the energy intake rate (E_a) and the maintenance requirements (E_m; app. A) per unit of time:

$$E_g(x, y) = E_a(x) - E_m(x, y). \tag{1}$$

We assume that the energy intake rate E_a depends on the irreversible mass x (Persson et al. 1998) and the availability of conspecific prey and alternative food (table 1). In case the energy intake exceeds the needs for maintenance, the surplus (E_g) is allocated to increase in irreversible and reversible mass following a rule that is described in detail in appendix A. The most important feature of the allocation rule is that as an individual grows, the ratio y/x asymptotically approaches a limit, which is q_J for juveniles and q_A for adults. In case the energy intake does not suffice to cover the requirements for maintenance (i.e., when $E_g < 0$), the individual starves and converts reversible mass into energy for maintenance. Starvation mortality occurs when the ratio y/x drops below a critical value, referred to as q_s. Then the individual suffers an additional mortality rate μ_s, which increases to infinity as the reversible mass y approaches zero:

$$\mu_s(x, y) = \begin{cases} s(q_s x/y - 1) & \text{if } y < q_s x \\ 0 & \text{otherwise,} \end{cases} \tag{2}$$

where s is a constant. The cannibalistic mortality rate μ_c will be discussed in detail below. A constant background mortality rate, μ_0, incorporates other causes of death. Together, these three rates sum up to the total mortality rate, μ:

$$\mu(x, y) = \mu_0 + \mu_s(x, y) + \mu_c(x). \tag{3}$$

It is commonly observed that perch mature at a specific size rather than a specific age (Alm 1952; Thorpe 1977; Treasurer 1981). In our model, we assume that an individual becomes adult when it reaches the maturation size

x_f. An adult is assumed to allocate a larger proportion of its surplus energy to reversible mass than a juvenile. Therefore the maximum ratio of reserves over structural mass for an adult (q_A) is assumed to be larger than that for a juvenile; that is, $q_A > q_J$ (app. A). The reversible mass, y, of an adult consists of both somatic reserves and gonads. We assume that the maximum amount of somatic reserves that an adult can attain is $q_J x$ and that the amount of reversible mass it has on top of this is gonad mass. Hence the amount of gonad tissue equals $(y - q_J x)$. A consequence of this assumption is that an individual starves away gonad tissue before somatic reserves. Reproduction is assumed to take place at the first day of a year. At that time the accumulated gonad tissue is converted into eggs. The number of eggs, F, that an adult produces equals

$$F(x, y) = \begin{cases} k_r(y - q_J x)/w_b & \text{if } y > q_J x \\ 0 & \text{otherwise,} \end{cases} \tag{4}$$

where k_r is a conversion factor that takes into account egg-respiration loss (15%) and loss of male gonad mass (35%), and where w_b is the mass of an egg.

The total production of newborns is the sum of the per capita fecundities of all adult individuals. Together, the young-of-the-year form a new cohort. They are assumed to be born at the same moment, with identical initial weight w_b and maximum condition ($y/x = q_J$). As long as they do not starve, these individuals have the maximum condition until they reach the maturation size. Because in our model all individuals in a cohort experience the same environmental conditions, their development is identical and therefore also their i-state at any future time. Thus, an important consequence of pulsed reproduction is that the population consists of discrete cohorts of identical individuals. In simulations, cohorts smaller than 10^{-9} individuals per liter ($\approx$one individual per lake) were considered extinct. Although in principle the number of cohorts in the population is unbounded, with this assumption the number of coexisting cohorts generally remained <20. Note that the number of cohorts may vary over time.

The i-state variables x and y and the functions that depend on them are, if necessary, indexed with respect to a specific cohort. For example, x_j refers to the irreversible mass of individuals in the jth cohort, where j may be any integer between 1 and the total number of cohorts. To parameterize processes that depend on body weight with data that are measured in total weight without knowing the ratio y/x, a standardized weight, referred to as w, is introduced. For an individual of a given length, w is defined as the maximum possible weight excluding gonad tissue; i.e., $w = x(1 + q_J)$. We assume that empirical data of individual total weight refer to this standardized weight.

Interactions: Planktivory and Cannibalism

The capacity to forage for zooplankton and conspecific prey changes during perch ontogeny. For example, larvae are efficient planktivores but cannot cannibalize, whereas very large individuals are poor planktivores but efficient piscivores. This ontogenetic niche shift is expressed in terms of attack rates, which are functions of body size.

The zooplankton attack rate is modeled as a hump-shaped function of w. It first increases with body weight, mainly due to increased mobility. A maximum attack rate $\hat{A}$ is reached at an optimal size, w_{opt}. The decrease of the attack rate can be related to a reduced ability to detect prey, as a consequence of decreased rod density. Following Persson et al. (1998), the zooplankton attack rate of a consumer with a standardized weight of w gram is described by

$$A_z(w) = \hat{A}\left[\frac{w}{w_{\mathrm{opt}}}\exp\left(1 - \frac{w}{w_{\mathrm{opt}}}\right)\right]^{\alpha}. \tag{5}$$

The exponent α determines how fast the attack rate increases with body size for small individuals. The population-dynamic implications of different values of α, $\hat{A}$, and w_{opt} are discussed in Persson et al. (1998). Experimental data on functional responses of differently sized perch show that equation (5) provides a good description of the size-dependent attack rate (Byström and Garcia-Berthóu 1999).

Modeling the cannibalistic interactions is complicated because the population of potential victims is size structured. Whether an individual classifies as prey for a potential cannibal depends on the lengths of both individuals (Popova and Sytina 1977; Willemsen 1977; Buijse and Van Densen 1992; Van Densen 1994; Christensen 1997; Mittelbach and Persson 1998). Experiments and field observations show that in perch, as well as in other piscivorous fish species, the victim has to be large enough to be detectable and small enough to be catchable (Eklöv and Diehl 1994; Christensen 1996; Lundvall et al. 1999; Persson et al. 2000). Figure 1 shows the length of the victim plotted against the length of the cannibal for observed cases of successful cannibalistic attack. The data are based on analysis of the stomach contents of perch from lakes (Persson et al. 2000) and on observations in experimental ponds and aquaria (Eklöv and Diehl 1994; Christensen 1996; Lundvall et al. 1999). From this figure we can infer that successful cannibalistic attacks occur when the combination of cannibal and victim length lies within a region roughly bordered by two straight lines (fig. 1). Drawn in the figure are the functions $v = \delta c$ and $v = \varepsilon c$, as a lower and an upper limit of this region, respectively. The vari-
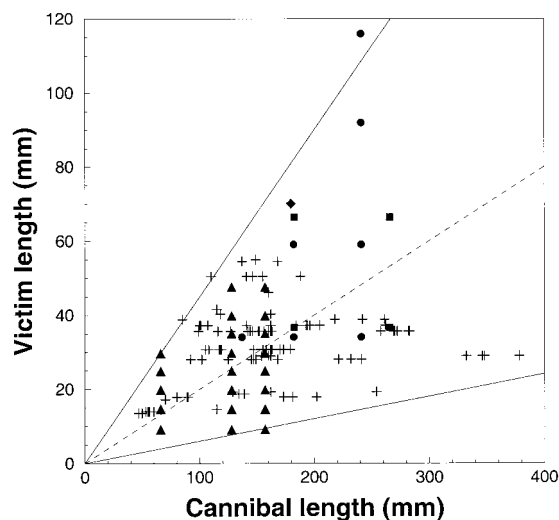
Figure 1: Victim length plotted against cannibal length for observed cases of successful cannibalistic attack in perch. Symbols refer to data from (*plus symbol*) Persson et al. 2000; (*filled triangle*) Lundvall et al. (1999); (*filled circle*) Christensen (1996); (*filled square*) B. Christensen, unpublished data; (*filled diamond*) Eklöv and Diehl (1994). The solid lines indicate the assumed lower limit ($v = \delta c$) and upper limit ($v = \varepsilon c$) of the size-dependent cannibalism window. The dotted line depicts the estimated optimal victim length ($v = \varphi c$) for a given cannibal length. Parameters are $\delta = 0.06$, $\varepsilon = 0.45$, and $\varphi = 0.2$.

ables v and c refer to the length of victim and cannibal, respectively, each being functions of irreversible mass (table 1). For a specific cannibal length, c, there is a window of victim lengths that are vulnerable to cannibalism ($\delta c < v < \varepsilon c$), which we refer to as the "cannibalism window." Christensen (1996) suggests that the maximum prey size that a piscivore can capture, and hence the upper limit of the cannibalism window, is determined by the swimming speed of both victim and cannibal. Supported by results from laboratory experiments (Lundvall et al. 1999), we assume that the optimal victim length is a fixed proportion, φ, of the cannibal length; that is, $v = \varphi c$, with $\delta < \varphi < \varepsilon$. The dashed line between the upper and lower limits in figure 1 indicates an estimate of this optimal victim length.

To complete the description of the cannibalistic attack rate, we assume that its absolute value equals the product of a maximum and a relative attack rate. The maximum attack rate is the attack rate for victims of the optimal size, $v = \varphi c$. We assume it to be an allometric function that increases deceleratingly with cannibal length, given by βc^{σ}, where $\sigma < 1$. The relative attack rate accounts for non-optimal victim sizes. From the optimal victim length $v = \varphi c$, it decreases linearly with victim length v from 1 to 0 at the boundaries of the cannibalism window. Over the

cannibalism window the relative attack rate thus resembles a tent function. In summary, the cannibalistic attack rate can be expressed as

$$A_c(c, v) = \begin{cases} \beta c^\sigma \dfrac{v - \delta c}{(\varphi - \delta)c} & \text{if } \delta c < v \leq \varphi c \\ \beta c^\sigma \dfrac{\varepsilon c - v}{(\varepsilon - \varphi)c} & \text{if } \varphi c < v < \varepsilon c \\ 0 & \text{otherwise,} \end{cases} \quad (6)$$

with parameters δ, ε, and φ as discussed above. The coefficient β scales the entire cannibalistic attack rate linearly. It is referred to as the cannibalistic voracity and will be varied to study the effect of cannibalism. For $\beta = 0$ the system reduces to a noncannibalistic consumer-resource system, analogous to the one studied by Persson et al. (1998).

We assume that an individual in the ith cohort encounters zooplankton prey mass at a rate that equals the product of its attack rate $A_z(w_i)$, the resource density R, and the weight of a prey item m:

$$\eta_z(x_i) = A_z(w_i)Rm. \quad (7)$$

We use $\eta_z(x_i)$ to denote the zooplankton mass-encounter rate. The encounter rate with potential victims in terms of victim biomass is a similar expression but summed over all potential victim cohorts. This mass-encounter rate is denoted as $\eta_c(x_i)$:

$$\eta_c(x_i) = \sum_j A_c(c_i, v_j)(x_j + y_j)N_j. \quad (8)$$

Here, $(x_j + y_j)$ refers to the total weight of a victim from the jth cohort, N_j to the density of the jth cohort, and A_c to the cannibalistic attack rate as defined in equation (6). The total encounter rate with prey mass equals the sum of the two resource specific rates, $\eta(x_i) = \eta_z(x_i) + \eta_c(x_i)$. The actual intake rate is assumed to be limited by the capacity to process food. An allometric function $H(w)$ describes the digestion time per gram of prey mass for an individual with standardized weight w (app. B):

$$H(w) = \xi_1 w^{\xi_2}. \quad (9)$$

Because gut size increases with body size, this digestion time is a decreasing function of body size, and thus $\xi_2 < 0$. The total mass intake rate $I(x_i)$ is described by a Holling Type II functional response dependent on the total mass-encounter rate and irreversible mass:

$$I(x_i) = \frac{\eta(x_i)}{1 + H(w_i)\eta(x_i)}. \quad (10)$$

The rate at which individuals fall victim to cannibalism can be derived from the density of cannibals, their cannibalistic attack rate, A_c, and their functional response. The per capita cannibalistic mortality rate, μ_c, in cohort j is

$$\mu_c(x_j) = \sum_i \frac{A_c(c_i, v_j)N_i}{1 + H(w_i)\eta(x_i)}, \quad (11)$$

in which N_i is the density of the potential cannibal cohort i.

The planktivorous predation pressure imposed on the resource population can be calculated analogously to the cannibalistic mortality rate. We assume that in the absence of planktivory, the zooplankton population grows following semichemostat dynamics. Semichemostat resource dynamics may be more applicable than the commonly used logistic growth resource dynamics when the resource has a physical refuge and includes invulnerable, smaller (albeit mature) size classes that grow into vulnerable size classes, as is the case with zooplankton fed upon by planktivorous fish (Persson et al. 1998). The resource dynamics are hence described by

$$\frac{dR}{dt} = r(K - R) - R\sum_i \frac{A_z(w_i)N_i}{1 + H(w_i)\eta(x_i)}, \quad (12)$$

where $A_z(w_i)$ is the per capita planktivorous attack rate of a perch in cohort i, $H(w_i)$ is the digestion time, $\eta(x_i)$ is the total mass-encounter rate, and N_i is the density of individuals in this cohort.

Results

The dynamics of our model were studied with a numerical method for the integration of physiologically structured population models called the "Escalator Boxcar Train" (De Roos et al. 1992; De Roos 1997). In the presentation of our results, individuals are referred to by their age in integer years with a + added; for example, young-of-the-year individuals are referred to as 0+. The term "juveniles" indicates immature individuals who are at least 1 yr old; it excludes the 0+, whereas "adults" refers to mature individuals.

The Baseline Case: No Cannibalism

First, we consider the case without cannibalism ($\beta = 0$).

β=0
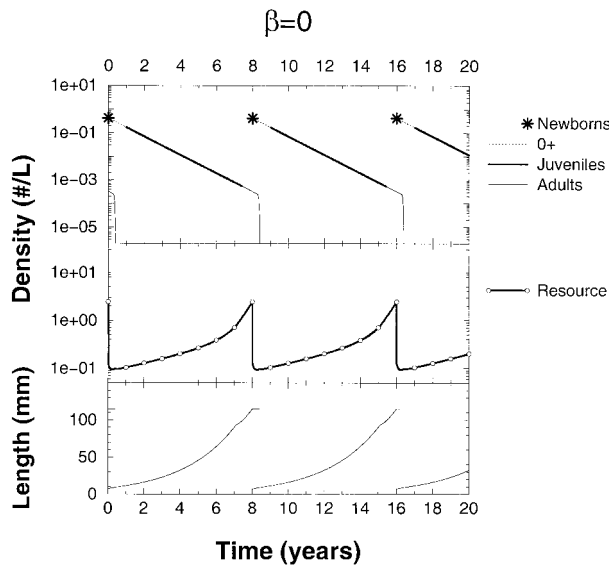
Figure 2: Time series of the population dynamics predicted by the model for the case without cannibalism ($\beta = 0$) showing single-cohort, recruit-driven cycles. All densities are in #/L. *Upper panel*, consumer density. *Asterisk*, pulse of newborns. *Dashed line*, density of 0+ individuals. *Thick line*, density of juveniles ≥1 yr old. *Thin line*, density of adults ≥1 yr old. The transition of the thick line into a thin line marks the maturation of all individuals. *Middle panel*, resource population density. *Open circles*, resource density at the first day of the year (spring). *Lower panel*, growth trajectories (length in mm) of all present cohorts. Parameters are as in table 2.

It is useful to note that for an individual of irreversible mass x and reversible mass $y = q_J x$, there is a critical resource density for which the energy intake rate exactly balances the metabolic rate; that is, $E_a(x) = E_m(x, q_J x)$. With the parameters for perch feeding on zooplankton (table 2), the critical resource level increases monotonically with body size. This implies that smaller individuals can sustain themselves on a lower resource level than larger ones. Consequently, a numerous cohort of small individuals (e.g., a pulse of newborns) may out-compete a cohort of larger individuals (e.g., their parents) through exploitative competition. Persson et al. (1998) predict that this situation leads to strong fluctuations with only a single cohort present, so-called recruit-driven cycles.

A time series of the recruit-driven population dynamics for the case without cannibalism is illustrated in figure 2. Once every 8 yr, a large pulse of newborns is produced that depresses the resource density to a level just above their own critical resource level. This resource density is below the level that adults need to cover their maintenance metabolism. Thus, adults starve to death when the 0+ are almost 4 wk old. Because of the constant yearly survival of 40%, set by the background mortality, the juvenile den-

sity declines exponentially. The individuals grow slowly at the beginning of the cycle, when their density is still high and, consequently, the resource density is low (fig. 2). Since maturation, at the age of 7+, occurs in the beginning of the season, the matured individuals have plenty of time to accumulate gonad tissue and to give rise to another strong reproductive pulse, which starts the cycle all over again.

Analysis of the resource dynamics shows that throughout the cycle the resource population is in pseudo–steady state with the current consumer density. As the consumers grow in size (fig. 2), their per capita foraging capacity increases (eqs. [5], [9]). Yet total-population foraging pressure on the resource decreases over time because consumer density decreases sufficiently fast. Hence the resource density increases over time. At the individual level, the joint effect of an increase in both foraging capacity and resource availability is that the per capita consumption rate, as well as the individual growth rate, increase during the cycle (fig. 2).

Increasing the Cannibalistic Voracity

We will study the effect of cannibalism by gradually increasing parameter β, cannibalistic voracity. Figure 3 shows a bifurcation diagram that summarizes the asymptotic
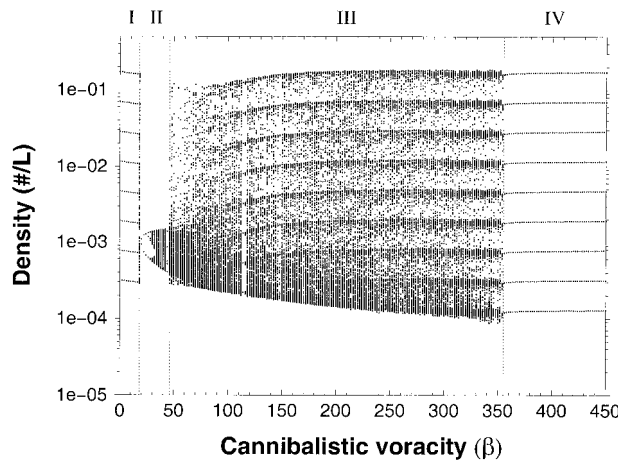
Figure 3: Bifurcation diagram with cannibalistic voracity (β) ranging from 0 to 450. Other parameters are as in table 2. For any value of β, the model was run for 500 yr, and the population state was sampled during the last 250 yr. The figure shows the population state at the first day of each year in each run. Each dot represents the number of individuals per liter, excluding the young-of-the-year (0+). Roman numerals refer to the four regions with different patterns of population dynamics (see "Results"). The 8-yr cycle in region I, for example, is represented by eight points, denoting the population density in 8 consecutive years.

population dynamics of the system for values of β between 0 and 450. Four distinct regions can be distinguished. In region I ($0 < \beta \lesssim 19$), the population cycles through eight points, as described above for the case $\beta = 0$. In region II ($19 \lesssim \beta \lesssim 45$), the population cycles with a small amplitude, going through a series of period doublings as β is increased. In region III ($45 \lesssim \beta \lesssim 355$), dynamics are irregular, alternating between phases with large and small amplitude cycles, respectively. Finally, in region IV ($\beta \gtrsim 355$), the population cycles regularly through nine points with a large amplitude.

To check for alternative stable dynamics, simulations were carried out for the same value of β using different initial states. Although the time to reach an attractor may vary considerably, the system always showed the same asymptotic dynamics; hence there is no evidence of alternative stable states. Each of the four regions will be discussed in detail below, starting with the regular patterns in regions I, II, and IV.

Region I: Recruit-Driven Cycles. The system exhibits recruit-driven, 8-yr cycles for values of β in region I. Because the adults cannibalize the newborns, the $0+$ cohort temporarily suffers an additional, cannibalistic mortality that causes a faster decline of its density. Since the recruits control the resource, an indirect result of cannibalism is a slightly increased resource level and an increased individual growth rate for recruits. Consequently, the juveniles mature earlier in the year (at the age of $7+$) and have a longer period until the next spring to accumulate gonad tissue. Thus, through the indirect effect on the growth rate, a higher cannibalistic voracity leads to earlier maturation, which in turn leads to increased per capita fecundity. The large pulse of newborns, which drives the cycle, is maintained by the increased per capita fecundity, despite the decreased density of mature individuals. For a sufficiently high cannibalistic voracity, the juveniles grow fast enough to mature at the age of $6+$, just before the end of the year. At this point the recruit-driven, 8-yr cycle destabilizes (fig. 3).

Region II: Small-Amplitude Cycles. When the recruit-driven cycles disappear ($\beta \approx 19$), a totally different pattern emerges, characterized by small oscillations and by the absence of severe resource depletions (fig. 4). Mature individuals are continuously present in the population and produce pulses of newborns yearly. Because the newborns are cannibalized by the other cohorts, the total population remains relatively small and the resource density relatively high. The density of juveniles, adults, and resources fluctuates in an approximately 2-yr cycle. Survival of $0+$ varies with a 2-yr period, causing an alternation of strong (more abundant) and weak (less abundant) cohorts. Due to the
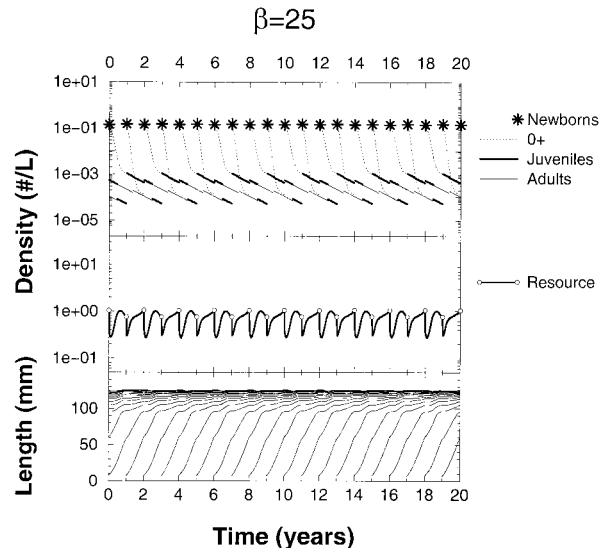

Figure 4: Time series of the population dynamics predicted by the model for $\beta = 25$, showing small-amplitude cycles with a period of 2 yr. *Upper panel*, dynamics of the cannibalistic consumers, showing the alternation of weak and strong cohorts. A faster decline of $0+$ (*dashed line*) indicates a higher cannibalistic mortality rate. Where trajectories end at nonzero densities, the individuals age or mature into the next class. *Middle panel*, resource population. *Lower panel*, lengths of all present consumer cohorts. Symbols are as in figure 2; parameters are as in table 2.

relatively constant resource density, individuals show a concave growth trajectory up to an asymptotic size, where energy intake balances metabolic needs. This ultimate size is determined by the density of the alternative resource and is not significantly increased by the cannibalistic energy gain. Because the resource density is high, individuals grow fast, reaching maturity in their second year.

Figure 5 shows that only the newborn cohort is cannibalized and that all other year classes contribute to the cannibalistic mortality of the $0+$. The snapshots also illustrate the alternation of weak and strong $1+$ year classes. When the $1+$ cohort is weak (e.g., at $T = 2$), it imposes a low cannibalistic mortality on $0+$ individuals, and vice versa when the $1+$ cohort is strong. Individuals reach the maturation size at the age of $1+$, but more abundant cohorts mature later in the season than less abundant cohorts due to intracohort competition.

The bifurcation diagram (fig. 3) shows that as β is increased in region II, the cycle is destabilized through a series of period doublings, while the amplitude of the cycle increases slowly. Although the size distribution becomes less regular as β is increased, the population-dynamic pattern remains essentially the same. With more voracious cannibalism, the difference between the density of strong and weak cohorts becomes more pronounced, as does the

β=25
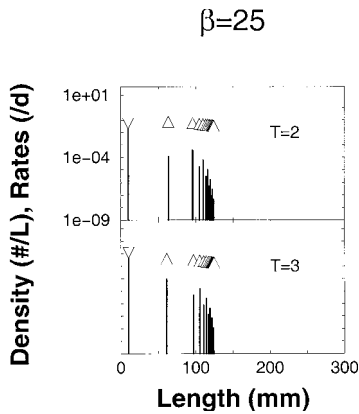
Figure 5: Length distribution of the cannibalistic consumer population at the tenth day of 2 consecutive years in the small-amplitude cycles for β = 25, corresponding to the time series in figure 4. Each bar represents a cohort of identical individuals. The population consists of 13 cohorts: from left to right, one newborn (0+), one juvenile (1+), and 11 adult (2+, 3+, etc.) cohorts. Additional symbols: *open inverted triangle*, per capita cannibalistic mortality rate, μ_c (per day); *open triangle*, per capita cannibalistic intake rate (g/d). Note that only the youngest cohort is cannibalized but that all other cohorts cannibalize.

variation in their age at maturity. At the value of β where the age at maturity of a strong cohort may exceed 2 yr, the small-amplitude cycle is disrupted by an incidental, very large pulse of newborns that depletes the resource. Beyond this value of β (region III), the small-amplitude cycles are unstable.

Region IV: Dwarfs-and-Giants Cycles. In region IV a regular 9-yr cycle is found that is characterized by the coexistence of two size classes, referred to as "dwarfs" and "giants," respectively, which differ in growth rate, maximum body size (fig. 6), and diet. The dwarfs are mainly planktivorous throughout their lives, whereas the giants shift from planktivory, via a mixed diet, to pure cannibalism. This enables them to reach body weights of up to 10 times the maximum body weight of a dwarf.

Figure 6 shows a time series of the population dynamics for β = 360. A striking feature is the pattern of reproduction: two strong pulses of newborns are followed by a series of small pulses. The figure shows that a single size class matures shortly after $T = 6$ and produces the first strong pulse of newborns at $T = 7$. Intense cannibalism during a short period decreases the density of the 0+ individuals dramatically, which in turn leads to a quick recovery of the resource (fig. 6) and prevents starvation of adults. Under such abundant food conditions, the surviving 0+ grow very fast (fig. 6) and mature just after $T = 8$, when the second strong pulse is produced. The constant, exponential decline of the cohort born at $T = 8$ shows that

these individuals suffer neither starvation nor cannibalistic mortality. Consequently, the resource does not recover, and most adults starve to death. While the density of the few survivors of the cohort born at $T = 7$ declines exponentially due to background mortality, they produce small pulses of offspring each year, which have no significant impact on the resource dynamics.

A closer inspection of the population structure (fig. 7) reveals the mechanism behind this pattern of population dynamics. The adults that cannibalized the 0+ cohort at $T = 7$ have become too big to "see" the newborns at $T = 8$ (fig. 7). Shortly after $T = 8$, the 0+ deplete the resource population (fig. 6) and outcompete the large cannibals before becoming vulnerable to them. Meanwhile, this strong 0+ cohort induces a shift from planktivory to piscivory in the 1+ adults. Although cannibalism by the few 1+ has a negligible effect on 0+ mortality (fig. 7, $T = 8$), the cannibalistic energy gain enables the 1+ to

β=360
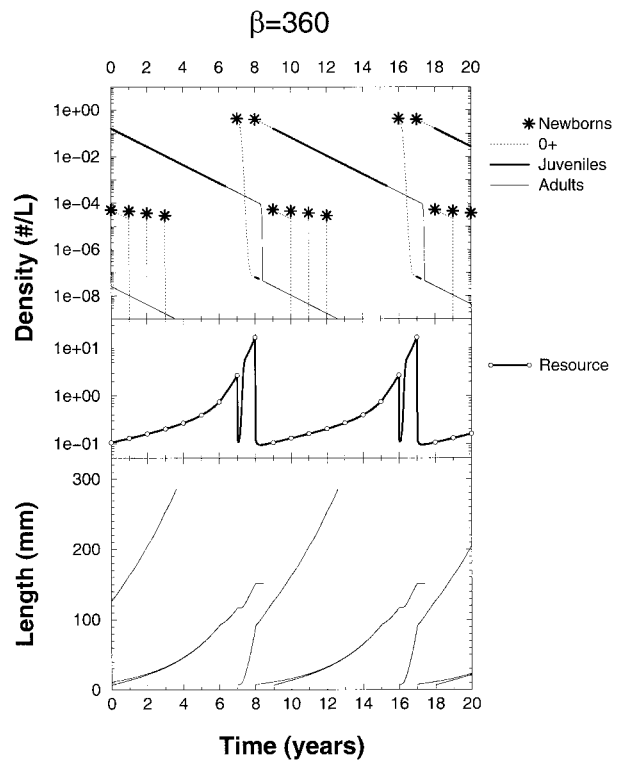
Figure 6: Time series of the dwarfs-and-giants cycle for β = 360. *Upper panel*, dynamics of the cannibalistic consumer population, showing the characteristic pattern of reproduction and the drop in the adult density. Where trajectories end at nonzero densities, the individuals age or mature into the next class. For example, at $T = 8$, 9, and 10, the dashed line disappears because the cohort ages into the juvenile class. *Middle panel*, resource population. *Lower panel*, lengths of all present consumer cohorts. Symbols are as in figure 2; parameters are as in table 2.

β=360
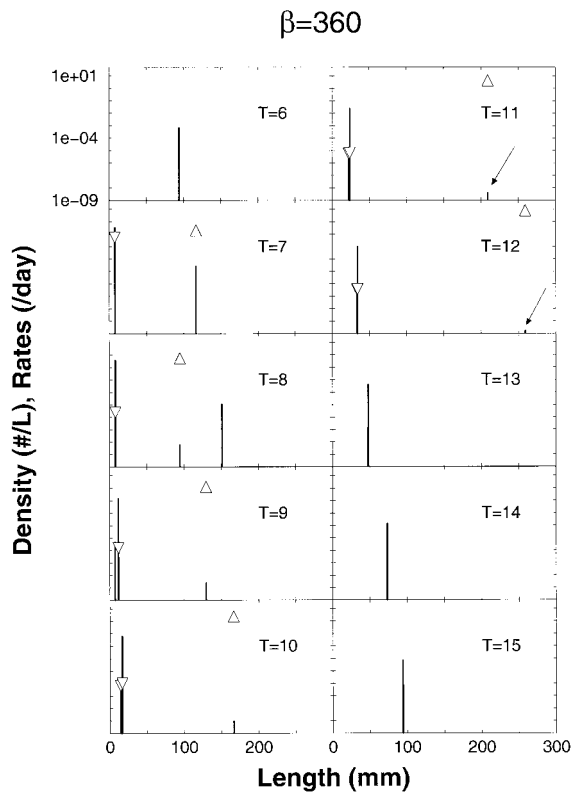
Figure 7: Length distribution of the cannibalistic consumer population sampled at the tenth day of 10 consecutive years during the dwarfs-and-giants cycle for $\beta = 360$, corresponding to figure 6. Each bar represents a cohort of identical individuals. Other symbols: *open inverted triangle*, per capita cannibalistic mortality rate; *open triangle*, per capita cannibalistic consumption rate. Note that at $T = 8$ the longer adults are too long to cannibalize the newborns, whereas at $T = 7$ they imposed a high cannibalistic mortality on the 0+. At $T = 11$ and 12 the arrows indicate the giants. The population state at $T = 15$ is identical to the state at $T = 6$.

survive the resource depletion. For obvious reasons (fig. 6), the few survivors of the first strong pulse of newborns will be referred to as giants, while the second strong pulse will be referred to as dwarfs.

The dwarfs are the main food source of the giants. Because the density of dwarfs decreases exponentially as a result of background mortality (fig. 6), the growth and even the survival of the giants is possible only if the dwarfs grow at a suitable rate. As the dwarfs grow, they become more vulnerable and contain more energy per individual. They should grow fast enough to ensure a sufficient energy intake for giants. Yet they should grow slow enough (relative to the giants' own growth rates) not to escape from the giants' cannibalism windows. Since the growth of giants is induced by the growth of their victims, the giants can be said to "surf" on a wave of dwarfs.

The planktivorous dwarfs drive the cycle like the recruits drive the cycles in region I (fig. 2), that is, the dwarfs control the resource population because of their abundance, keeping the resource density close to their own critical resource level. As a result, the growth trajectory of the dwarfs is similar to that of the recruits in the recruit-driven cycles (fig. 2). Due to their abundance, the dwarfs also dominate overall population fecundity; the majority of individuals in both the giant and the dwarf cohorts are the offspring of the previous dwarf cohort. Despite the high per capita fecundity of giants (up to 1.7×10^4 eggs vs. 3.3×10^3 for dwarfs), the total density of their offspring in the years $T = 9, \ldots ,12$ is low (fig. 6). Only a few offspring from the giants (born $T = 9$) converge to the dwarf size class; most offspring ($T = 10, \ldots ,12$) are cannibalized by dwarfs (fig. 6).

With more voracious cannibalism (even $\beta > 450$), the cycle remains qualitatively the same, although the density of giants that survive cannibalism following the first strong pulse of newborns is smaller. At a high value ($\beta \approx 1500$), the population goes extinct.

Region III: Mixed Dynamics. In region III there is no regular population-dynamic pattern (fig. 3). Yet in time series, periods with dynamics that resemble small-amplitude cycles can be distinguished from periods with dynamics similar to dwarfs-and-giants cycles. An example of the population dynamics in this region is shown in figure 8, for $\beta = 100$. During the first 8 yr, the population dynamics resemble the small-amplitude cycles (cf. fig. 4); 0+ individuals grow fast toward an asymptotic size and mature in their first or second year, while a number of adult year classes is cannibalizing them. Compared to the small-amplitude cycles in region II (fig. 4), however, the fluctuations are irregular and have a large amplitude. The cannibalistic mortality rate of newborns fluctuates strongly from year to year, resulting in varying rates of decrease in the 0+ density (fig. 8). Also, the initial density of newborns fluctuates considerably from year to year.

Whenever a large pulse of newborns depresses the zooplankton resource below the critical level of the adults at the same time that the adults fail to cannibalize the newborns, the dynamics change in character (fig. 8; $T = 8$). The abundant juveniles keep the resource density close to their critical resource level and thus inhibit their own growth rate. In the years $T = 8, \ldots ,14$ the dynamics resemble a dwarfs-and-giants cycle (cf. fig. 6). The sudden drop in the adult density at $T = 8$ indicates that a majority of the adults starve to death because of resource depletion. The remaining adults, which belong to two different cohorts, switch to cannibalism. As individuals in the juvenile size class ("dwarfs") grow slowly in size, growth of the adults accelerates, and the adults become giants (fig. 8).

β=100
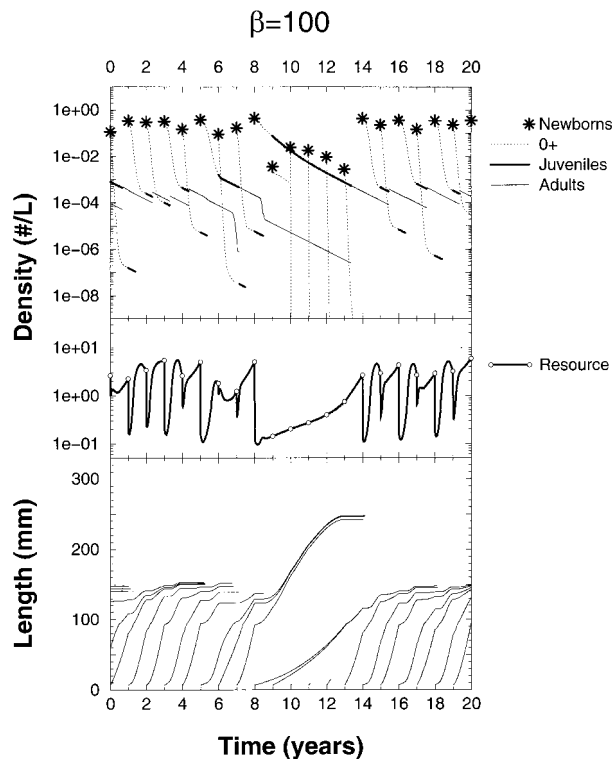
Figure 8: An example of the mixed dynamics in region III. The population dynamics predicted by the model for $\beta = 100$ resemble small-amplitude cycles before $T = 8$ and after $T = 14$ and a dwarfs-and-giants cycle from $T = 8$ to 14. *Upper panel,* cannibalistic consumer density. *Middle panel,* resource density. *Lower panel,* lengths of all present consumer cohorts. Symbols as in figure 2; parameters as in table 2.

When the dwarfs are mature and reproduce (at $T = 14$), the system starts to fluctuate with a small amplitude again.

The dynamics have been studied on longer time intervals for various values of cannibalistic voracity (β) within region III. Independent of the value of β, the transition from periods resembling small-amplitude cycles to dwarfs-and-giants cycles is initiated by a successful 0+ cohort that depresses the resource for a prolonged period. For higher values of β, the resource and population densities tend to change more dramatically at such transitions. The simulations also show that the fraction of time that the system fluctuates with a small amplitude decreases while the dwarfs-and-giants cycles become more stable. The dominant period of the fluctuations gradually increases from 2 to 9 yr when β is increased. Both the growth rate and the ultimate length that the giants attain increase with β because the intake rate from cannibalism increases.

Parameter Sensitivity

We have studied the sensitivity of the system to changes in the parameters of resource dynamics (K, r), individual physiology (q_J, q_A, λ_1, λ_2, ξ_1, ξ_2), and the cannibalism window (δ, ε, φ). Changing these parameters has mainly a quantitative effect. The same population-dynamic patterns, including growth trajectories, are obtained, but transitions between regions occur at different parameter values. For example, the transition between regions III and IV shifts to higher β values as either K or δ is increased. The system is most sensitive to the parameter δ because ξ determines whether newborns are within or outside the cannibalism window of adults, which is crucial to dwarfs-and-giants cycles.

Preliminary results from pond experiments suggest that the cannibalistic voracity of perch lies in a range of $100 \lesssim \beta \lesssim 200$ (B. Christensen, unpublished data). We conclude that with parameter values realistic for perch (table 2), the four regions, and especially region III, occur in a plausible range of β.

Discussion

The Interplay between Size-Dependent Cannibalism and Competition

Our analyses show that the combination of size-dependent cannibalism and competition yields results that were hard to expect on the basis of knowledge of either interaction separately. The most striking example is the case where, in a certain phase of a population cycle, cannibalism lifts a few individuals beyond the asymptotic size determined by alternative food, resulting in "double" growth curves. Although it has been shown that cannibalism may have a positive effect on a cannibal's growth rate (DeAngelis et al. 1979; Simon 1984; Wilbur 1988; Fagan and Odell 1996; Maret and Collins 1997), the mechanism of such a population-dynamic bottleneck has not been demonstrated before.

In intraspecific competition, smaller individuals are often superior to larger ones because of size-dependent scaling of foraging and metabolic rates (Persson 1987; Werner 1988; Persson et al. 1998). In the absence of cannibalism, such intercohort competition causes recruit-driven, single-cohort cycles (Persson et al. 1998). The mechanism that causes the cycles implies that resource density increases during the cycle. Given the size-dependent foraging and metabolic rates, as found in laboratory experiments, this results in an accelerating growth rate (fig. 2). Examples of recruit-driven cycles are given in Persson et al. (1998) and include the fish species roach (*Rutilus rutilus*) and cisco (*Coregonus albula*). Despite evidence of intercohort competition (Persson 1987), recruit-driven cycles or accelerating growth curves are not found in perch (e.g., see below). We therefore hypothesize that the presence of other interactions, such as consumption of a second re-

source (macroinvertebrates) or cannibalism, interferes with size-dependent competition. We investigate the effect of cannibalism in this article, while the influence of a second resource will be the subject of future research. Note, however, that the accelerating growth curves are not essential to the effects of cannibalism that we find because analogous results are obtained with a continuous-time model where the growth curves are decelerating (see below; fig. 9).

Our results show that cannibalism may serve as a mechanism by which larger individuals compensate for their competitive inferiority to smaller individuals. When cannibalistic voracity is moderate (region II; fig. 3), the single-cohort cycles disappear and the population reaches a state with a large, slightly fluctuating adult size class that consists of many cohorts (figs. 4, 5). Although many eggs are produced each year, many of the 0+ are cannibalized. This stabilizing effect is, however, not unique to cannibalism since the same result could be obtained by other mechanisms that cause a high mortality of young-of-the-year. Such size-dependent mortality could result from, for instance, infanticide (Hausfater and Hrdy 1984), size-dependent predation risk (Tripet and Perrin 1994), interference competition (Borgström et al. 1993), or sensitivity to starvation (Post and Evans 1989). Similar results were found by Cushing (1991) and also by Van den Bosch and Gabriel (1997). The latter found that cannibalism dampens single-generation cycles in an age-structured population model.

With more voracious cannibalism (region IV; fig. 3), the interplay between size-dependent cannibalism and competition generates a bimodal size distribution (fig. 7). Individuals in the two modes of this distribution, referred to as dwarfs and giants, respectively, are characterized by two very different life histories, which result from a reversal in importance of cannibalism and competition. Whether individual growth is determined by competition or cannibalism depends on the population structure at the time of birth. Shortly after birth, the cohort of individuals that will become giants is almost entirely wiped out as a result of cannibalism by older cohorts. Intracohort competition is thus negligible, and such individuals grow very fast. The giants are forced to switch to cannibalism in their second year and manage to grow beyond the asymptotic length set by a planktivorous diet. The growth of dwarfs, on the other hand, is inhibited by severe intracohort competition, since their abundance is not decreased by cannibalism. Because the giants "surf" on the dwarf size class, growth of giants is possible only if the dwarfs grow at a suitable rate. Without the severe intracohort competition, such as in small-amplitude cycles (fig. 4), victims grow too fast to support giants (cf. fig. 8; $T = 15$). Hence, cannibalism and
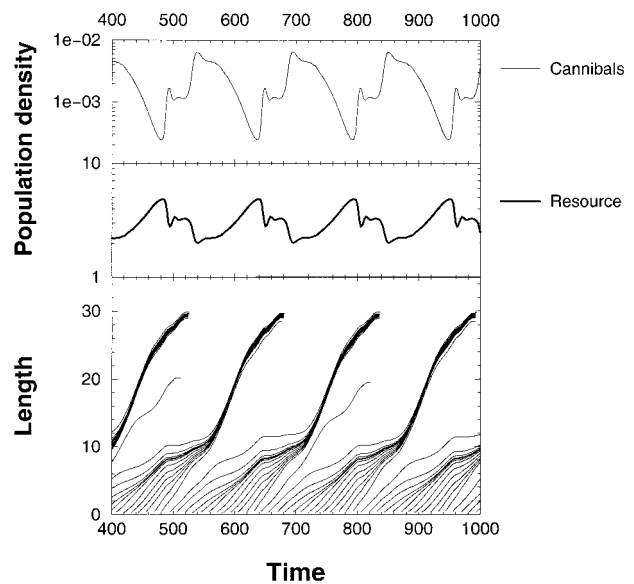

Figure 9: Dynamics predicted by the continuous-time Kooijman-Metz model with size-dependent cannibalism (see "Discussion"). *Upper panel*, total population density of cannibalistic consumers. *Middle panel*, resource density. *Lower panel*, individual growth curves (not all cohorts are shown). Note the divergence of lengths between "dwarfs" and "giants" at $T = 490$, 645, and 800. Individuals that are born slightly later are inhibited by competition and grow slowly, whereas the slightly older individuals grow more quickly as a result of cannibalistic energy gain and become giants.

competition together cause the typical phenomenon of dwarfs-and-giants cycles.

The analyses to test model sensitivity showed that the different types of dynamics that are found with the default parameters for perch are robust to changes in parameter values. As a more far-reaching test of the robustness of the results to the assumptions of our model, we investigated a strongly simplified variant of it, which is basically a Kooijman-Metz model (Kooijman and Metz 1984; De Roos et al. 1992) extended with size-dependent cannibalism (D. Claessen and A. M. DeRoos, unpublished manuscript). This model of a continuously reproducing, structured population has a single *i*-state variable (length ℓ) and is based on the assumption that individuals have a linear functional response; that food intake scales with body surface ($\propto \ell^2$); that metabolic rate scales with total body weight ($\propto \ell^3$); that a fraction of assimilated energy is allocated to reproduction; and that the cannibalistic attack rate is a continuous, smooth, dome-shaped function of the ratio of cannibal to victim length. The emergence of dwarfs and giants in the population dynamics predicted by this model (fig. 9) shows that the phenomenon is not a product of the specific assumptions of the perch model, such as the energy allocation rule, discrete reproduction,

or a Type II functional response. On the contrary, it suggests that the phenomenon is bound to occur more generally in populations with both size-dependent cannibalism and competition.

In this study we do not consider intracohort cannibalism. Yet, in case an intracohort size distribution is wide enough to allow for cannibalism (cf. fig. 1), it may lead to strongly diverging individual growth and survival rates (DeAngelis et al. 1979; Fagan and Odell 1996). A laboratory study with single cohorts of largemouth bass (*Micropterus salmoides*) showed that an entire year class may be decimated by such intracohort cannibalism, with the cannibals reaching much larger sizes than individuals in trials with a narrower size distribution (DeAngelis et al. 1979). On the other hand, the scope for intracohort cannibalism may be limited by a size-dependent growth rate. Intense competition among dwarfs, for instance, ensures that individuals grow toward a time-dependent, asymptotic size, which results in convergence of sizes. This is illustrated in figures 6 and 8, where the sizes of different cohorts converge quickly to the dwarf size class. Yet, it cannot be ruled out a priori that cannibalism enables an "intracohort giant" (cf. DeAngelis et al. 1979) to escape a first asymptotic size, which is set by competition for the alternative resource, and to converge toward a second asymptotic size, which is set by cannibalism. This possibility and its population-dynamic consequences remain to be investigated.

Model Results and Empirical Data on Population Dynamics

Le Cren (1992) observed "exceptionally big perch" in Lake Windermere, where perch usually reached an asymptotic length of approximately 18 cm. Yet, repeatedly, a small number of perch had a "double" growth curve with an ultimate asymptotic length of around 46 cm. These big perch were mainly piscivorous, feeding largely on smaller perch. Strikingly, most big perch accelerated their growth in years with large numbers of 0+ perch surviving, frequently followed by years when 0+ perch were scarce. Le Cren (1992) suggests that the big perch continued to feed on the cohort that initiated their acceleration, while both the cannibal and the victims grew larger (i.e., "surfing" on the cohort of smaller perch). The shape of the growth trajectories of the big perch, their diet, and timing of acceleration are hence in agreement with the giants predicted by our model (regions III and IV). Moreover, the cohorts that stimulated the growth of these big perch showed similarities with dwarf cohorts, that is, high density, reduced growth rate, and an exceptionally large contribution to following generations (Craig 1980). Double growth curves

have also been reported from other perch populations (McCormack 1965; Persson et al. 2000; see below).

Empirical field data on the effect of cannibalism and intercohort competition on population dynamics are rare, mainly because in many systems other interactions, like interspecific predation and competition, are also present. A notable exception is a study by Persson et al. (2000) of a perch population in a lake (Abbortjärn 3, central Sweden) where no other fish species are present. This study is of particular interest in this context because it includes detailed information on perch population density and its size structure, growth trajectories of individual perch, and resource levels. Figure 10 shows that in this lake, until 1994, the individuals reached a maximum length of approximately 180 mm. In 1994, however, some individuals that had reached the normal asymptotic length accelerated their growth, which resulted in "double" growth curves (fig. 10). Stomach content analyses showed that these individuals had a cannibalistic diet (Persson et al. 2000). The growth curves of these large individuals are strikingly similar to the growth curves of giants predicted by our model (fig. 6, 8).

The timing of the acceleration of the giants coincided with the first successful 0+ cohort, which served as a rich food supply just as in our model where in region III giants accelerated at the disturbance of small-amplitude cycles by a successful 0+ cohort. From 1991 until 1994, the population was dominated by an abundant size class of individuals that were 2–6 yr old and produced large pulses of 0+ each spring (fig. 11*A*). Despite high resource levels, annual survival of 0+ perch was very low, which resulted in a very low density of 1+ perch (fig. 11*A*). According to Persson et al. (2000), cannibalism by the perch ≥2 yr old caused the high mortality of 0+ in those years. The
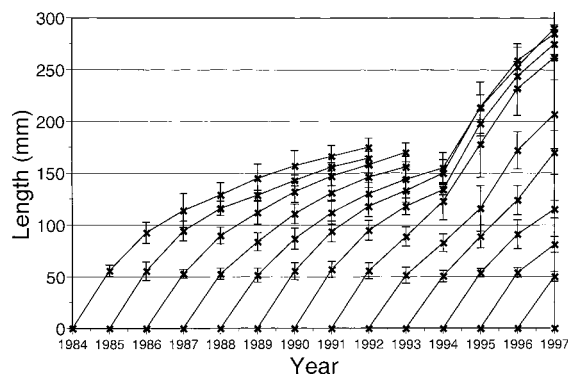
Figure 10: Back-calculated growth trajectories of different year classes in the studied perch population from 1985 to 1997 (from Persson et al. 2000).
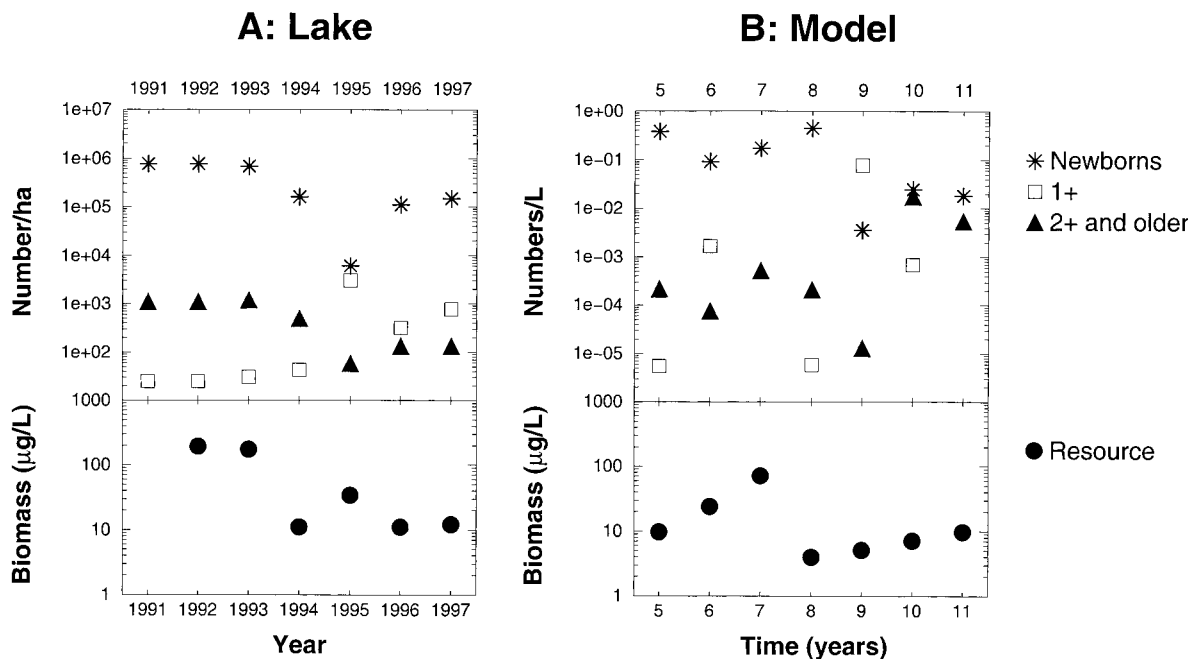
Figure 11: Comparison of population dynamics in the lake and population dynamics predicted by the model. *A, Upper panel,* dynamics of the studied perch population: spring (May) density (#/ha) of hatching newborns (*asterisk*), of 1+ perch (*open square*), and ≥2 perch (*filled triangle*) in the years 1991–1997. Annual 0+ survival can be deduced by comparing newborn density with 1+ density 1 yr later. *Lower panel,* summer (July–August) resource biomass (μg/L) during the period 1992–1997 in the studied lake. Data from Persson et al. (2000). *B,* Dynamics of the model for $\beta = 100$, showing $T = 5, \ldots, 11$ from the same time series as figure 8. *Upper panel,* density (#/L) newborns, 1+ and ≥2 perch at the first day of each year (spring). *Lower panel,* resource biomass (μg/L) halfway through each year (day 45; summer). Note that in the model only one prey size is considered, whereas the empirical data represents the sum of all present zooplankton species and size classes. The times, T, were chosen such that the breakthrough of a dense 1+ cohort (at $T = 9$ and in 1995, respectively) occurred in the middle of the time frame.

dynamics were hence reminiscent of the small-amplitude cycles occurring in regions II and III (figs. 4, 8). In 1994, this pattern was disrupted. The 0+ remained abundant throughout the year and depleted the resource population (fig. 11*A*). Persson et al. (2000) explained the high 0+ survival with reduced cannibalism by perch ≥2 yr old; the spring density of perch ≥2 yr old was only half that in the previous years (fig. 11*A*). Due to resource limitation, the majority of the perch ≥2 yr old starved to death before the spring of 1995. Individuals that survived the starvation had a "double" growth curve (fig. 10).

Based on the identical timing of the giants and supported by the preliminary estimate of $100 \lesssim \beta \lesssim 200$ for perch (B. Christensen, unpublished data), we compare the empirical data to our example of region III ($\beta = 100$; fig. 8) in more detail. The exact value of β is not relevant since the mechanism that caused acceleration is the same throughout region III. To facilitate comparison we have obtained the same population statistics from our model as those measured in the field (fig. 11*B*).

Comparison of the model results with the empirical data

shows striking similarities, both qualitatively and quantitatively. In both cases, the transition between the two patterns of dynamics was marked by a series of related events: a drop in the resource density (at $T = 8$ and in 1994) coinciding with a high 0+ annual survival ($T = 8$–9, 1994–1995); a drop in the density of perch ≥2 yr old (at $T = 9$ and in 1995), coinciding with a breakthrough of a dense 1+ cohort and a decrease in population fecundity. At $T = 8$ and in 1994, the sudden increase in 0+ annual survival coincided with the acceleration of giants (figs. 8, 10). This comparison suggests not only that the timing is identical but also that the mechanism responsible for the emergence of giants is the same in the lake as in our model. In our model, a high density of 0+ outcompetes most of the adults, whereas the few surviving adults use the 0+ as their main food resource and become giants. The data in figure 11*A* verify this interpretation for the lake as well.

After the acceleration of giants, however, there is an important discrepancy. In our model, the cohort born at $T = 8$ is not affected by competition with the cohorts born at $T = 9$, 10, and 11. In the lake, however, the competition

between 0+ and 1+ caused high mortality in the 1+ during the years 1995–1997 (but not 1998), despite the occurrence of cannibalism by 1+ (Persson et al. 2000). Whereas in our model the giants "surf" on the slowly growing dwarfs, in the lake the giants fed mainly on the successive young-of-the year, thus "jumping" from one 0+ cohort to the next. Several mechanisms may contribute to this discrepancy between our model and the data: the absence of a second resource (macroinvertebrates), for example, or the absence of size-dependent winter mortality. In the lake, winter mortality is considerably higher for 0+ than for older individuals (Persson et al. 2000).

In conclusion, the timing and the shape of the growth curves of the giants (fig. 10), together with the similarities between our model and the empirical data with regard to the transition in dynamics, provide strong support for our model as well as insight into the mechanism that induces giants in the lake. The comparison with the empirical data (fig. 11) also points out interesting aspects of the system that still warrant further investigations.

Acknowledgements

APPENDIX A

Assimilation and Energy Allocation

The ingested food is taken up with an efficiency, k_e, which incorporates assimilation efficiency and cost (specific dynamic action). Thus the energy intake rate equals

$$E_a(x) = k_e I(x). \tag{A1}$$

The metabolic demands for maintenance, E_m, depend on total body mass $(x + y)$. Based on the literature, we assume an allometric relationship (Beamish 1974; Kitchell et al. 1977):

$$E_m(x, y) = \rho_1 (x + y)^{\rho_2}. \tag{A2}$$

Assimilated energy is assumed to be allocated to reversible

and irreversible mass according to the following rule: if the energy intake, E_a, exceeds the metabolic demands for maintenance, E_m, a fraction, f,

$$f(x, y) = \begin{cases} \dfrac{1}{(1 + q_J)q_J} \dfrac{y}{x} & \text{if } x \le x_f \\ \dfrac{1}{(1 + q_A)q_A} \dfrac{y}{x} & \text{if } x > x_f \end{cases} \tag{A3}$$

of the surplus energy, E_g (eq. 1), is allocated to growth in irreversible body mass and the residual fraction to growth in reversible mass.

APPENDIX B

The Digestion Time

The size-dependent digestion time can be estimated from feeding experiments performed under excessive food conditions, where the intake rate can be assumed to be close to its maximum; that is, $I \approx I_{max}$. From the assumption that weight increment equals net ingestion $(\Delta W = k_e I_{max} - E_m$; see table 1) and the assumption that maximum intake rate equals the inverse of the digestion time per unit of prey weight, the handling time can be estimated as

$$H(w) = k_e / [\Delta W(w) + E_m(w)]. \tag{B1}$$

Using this relation, an allometric function for the size-dependent handling time was fitted to data from feeding experiments with perch (Lessmark 1983; Byström and Garcia-Berthóu 1999),

$$H(w) = \xi_1 w^{\xi_2}, \tag{B2}$$

with $\xi_1 = 5.0$ and $\xi_2 = -0.8$ (table 2).

Literature Cited

Alm, G. 1952. Year class fluctuations and span of life of perch. Report from the Institute of Freshwater Research, Drottningholm 33:17–38.

Anholt, B. R. 1994. Cannibalism and early instar survival in a larval damselfly. Oecologia (Berlin) 99:60–65.

Beamish, F. W. H. 1974. Apparent specific dynamic action of largemouth bass, *Micropterus salmonides*. Journal of the Fisheries Research Board of Canada 31:75–87.

Benoît, H. P., E. McCauley, and J. R. Post. 1998. Testing the demographic consequences of cannibalism in *Tribolium confusum*. Ecology 79:2839–2851.

Borgström, R., J. Heggenes, and T. G. Northcote. 1993. Regular, cyclic oscillations in cohort strength in an allopatric population of brown trout, *Salmo trutta* L. Ecology of Freshwater Fish 2:8–15.

Botsford, L. W. 1981. The effects of increased individual growth rates on depressed population size. American Naturalist 117:38–63.

Bragg, A. N. 1965. Further study of predation and cannibalism in spadefoot tadpoles. Herpetologica 20:17–24.

Buijse, A. D., and W. L. T. van Densen. 1992. Flexibility in the onset of piscivory and growth depensation in Eurasian perch, *Perca fluviatilis* L. Pages 89–121 *in* A. D. Buijse, ed. Dynamics and exploitation of unstable percid populations. Ph.D. diss. Wageningen Agricultural University, Netherlands.

Byström, P., and E. Garcia-Berthóu. 1999. Density dependent growth and size specific competitive interactions in young fish. Oikos 86:217–232.

Christensen, B. 1996. Predator foraging capabilities and prey antipredator behaviours: pre- versus postcapture constraints on size-dependent predator-prey interactions. Oikos 76:368–380.

———. 1997. Size refuges in predator-prey interactions. Ph.D. thesis. Umeå University, Sweden.

Costantino, R. F., R. A. Desharnais, J. M. Cushing, and B. Dennis. 1997. Chaotic dynamics in an insect population. Science (Washington, D.C.) 275:389–391.

Craig, J. F. 1980. Growth and production of the 1955 to 1972 cohorts of perch, *Perca fluviatilis* L., in Windermere. Journal of Animal Ecology 49:291–315.

Cushing, J. M. 1991. A simple model of cannibalism. Mathematical Biosciences 107:47–71.

———. 1992. A size-structured model for cannibalism. Theoretical Population Biology 42:347–361.

DeAngelis, D. L., D. K. Cox, and C. C. Coutant. 1979. Cannibalism and size dispersal in young-of-the-year largemouth bass: experiment and model. Ecological Modelling 8:133–148.

De Roos, A. M. 1997. A gentle introduction to physiologically structured population models. Pages 119–204 *in* S. Tuljapurkar and H. Caswell, eds. Structured-population models in marine, terrestrial, and freshwater systems. Chapman & Hall, New York.

De Roos, A. M., O. Diekmann, and J. A. J. Metz. 1992. Studying the dynamics of structured population models: a versatile technique and its application to *Daphnia*. American Naturalist 139:123–147.

Diekmann, O., R. M. Nisbet, W. S. C. Gurney, and F. van den Bosch. 1986. Simple mathematical models for cannibalism: a critique and a new approach. Mathematical Biosciences 78:21–46.

Dominey, W. J., and L. S. Blumer. 1984. Cannibalism of early life stages in fishes. Pages 43–64 *in* G. Hausfater and S. B. Hrdy, eds. Infanticide: comparative and evolutionary perspectives. Aldine, New York.

Dong, Q., and D. L. DeAngelis. 1998. Consequences of cannibalism and competition for food in a smallmouth bass population: an individual-based modeling study. Transactions of the American Fisheries Society 127: 174–191.

Eklöv, P., and S. Diehl. 1994. Piscivore efficiency and refuging prey: the importance of predator search mode. Oecologia (Berlin) 98:344–353.

Elgar, M. A., and B. J. Crespi, eds. 1992. Cannibalism: ecology and evolution among diverse taxa. Oxford University Press, New York.

Elliott, J. M. 1976. The energetics of feeding, metabolism and growth of brown trout (*Salmo trutta* L.) in relation to body weight, water temperature and ration size. Journal of Animal Ecology 45:923–948.

Fagan, W. F., and G. M. Odell. 1996. Size-dependent cannibalism in praying mantids: using biomass flux to model size-structured populations. American Naturalist 147:230–268.

Fincke, O. M. 1994. Population regulation of a tropical damselfly in the larval stage by food limitation, cannibalism, intraguild predation and habitat drying. Oecologia (Berlin) 100:118–127.

Fisher, M. E. 1987. An age-structured fish population model with coupled size and population density. Mathematical Biosciences 86:15–34.

Fox, L. R. 1975. Cannibalism in natural populations. Annual Review of Systematics and Ecology 6:87–106.

Gurney, W. S. C., and R. M. Nisbet. 1985. Fluctuation periodicity, generation separation, and the expression of larval competition. Theoretical Population Biology 28: 150–180.

Hastings, A. 1987. Cycles in cannibalistic egg-larval interactions. Journal of Mathematical Biology 24:651–666.

Hausfater, G., and S. B. Hrdy, eds. 1984. Infanticide: comparative and evolutionary perspectives. Aldine, New York.

Henson, S. M. 1997. Cannibalism can be beneficial even when its mean yield is less than one. Theoretical Population Biology 51:109–117.

Karås, P., and G. Thoresson. 1992. An application of a bioenergetics model to Eurasian perch (*Perca fluviatilis* L.). Journal of Fish Biology 41:217–230.

Kitchell, J. F., D. J. Stewart, and D. Weininger. 1977. Applications of a bioenergetics model to yellow perch (*Perca flavescens*) and walleye (*Stizostedion vitreum vi-*

treum). Journal of the Fisheries Research Board of Canada 34:1922–1935.

Kooijman, S. A. L. M., and J. A. J. Metz. 1984. On the dynamics of chemically stressed populations: the deduction of population consequences from effects on individuals. Ecotoxicology and Environmental Safety 8: 254–274.

Le Cren, E. D. 1992. Exceptionally big individual perch (*Perca fluviatilis* L.) and their growth. Journal of Fish Biology 40:599–625.

Lessmark, O. 1983. Competition between perch (*Perca fluviatilis*) and roach (*Rutilus rutilus*) in south Swedish lakes. Ph.D. diss. University of Lund, Sweden.

Lundvall, D., R. Svanbäck, L. Persson, and P. Byström. 1999. Size-dependent predation in piscivores: interactions between predator foraging and prey avoidance abilities. Canadian Journal of Fisheries and Aquatic Sciences 56:1285–1292.

Maret, T. J., and J. P. Collins. 1997. Ecological origin of morphological diversity: a study of alternative trophic phenotypes in larval salamanders. Evolution 51: 898–905.

McCormack, J. C. 1965. Observations on the perch population of Ullswater. Journal of Animal Ecology 34: 463–478.

Metz, J. A. J., and O. Diekmann. 1986. The dynamics of physiologically structured populations. Lecture Notes in Biomathematics 68. Springer, Berlin.

Mittelbach, G. G., and L. Persson. 1998. The ontogeny of piscivory and its ecological consequences. Canadian Journal of Fisheries and Aquatic Sciences 55:1454–1465.

Persson, L. 1987. The effects of resource availability and distribution on size class interactions in perch, *Perca fluviatilis*. Oikos 48:148–160.

———. 1988. Asymmetries in competitive and predatory interactions in fish populations. Pages 203–218 *in* B. Ebenman and L. Persson, eds. Size-structured populations: ecology and evolution. Springer, Heidelberg.

Persson, L., and L. A. Greenberg. 1990. Optimal foraging and habitat shift in perch (*Perca fluviatilis*) in a resource gradient. Ecology 71:1699–1713.

Persson, L., K. Leonardsson, M. Gyllenberg, A. M. de Roos, and B. Christensen. 1998. Ontogenetic scaling of foraging rates and the dynamics of a size-structured consumer-resource model. Theoretical Population Biology 54:270–293.

Persson, L., E. Wahlström, and P. Byström. 2000. Cannibalism and competition in Eurasian perch: population dynamics of an ontogenetic omnivore. Ecology 81.

Polis, G. A. 1981. The evolution and dynamics of intraspecific predation. Annual Review of Systematics and Evolution 12:225–251.

———. 1988. Exploitation competition and the evolution

of interference, cannibalism and intraguild predation in age/size-structured populations. Pages 185–202 *in* B. Ebenman and L. Persson, eds. Size-structured populations: ecology and evolution. Springer, Heidelberg.

Popova, O. A., and L. A. Sytina. 1977. Food and feeding relations of Eurasian perch (*Perca fluviatilis*) and pike-perch (*Stizostedion lucioperca*) in various waters of the USSR. Journal of the Fisheries Research Board of Canada 34:1559–1570.

Post, J. R., and D. O. Evans. 1989. Size-dependent overwinter mortality of young-of-the-year yellow perch (*Perca flavescens*): laboratory, in situ enclosure and field experiments. Canadian Journal of Fisheries and Aquatic Sciences 46:1958–1968.

Post, J. R., E. A. Parkinson, and N. T. Johnston. 1999. Density-dependent processes in structured fish populations: interaction strengths in whole-lake experiments. Ecological Monographs 69:155–175.

Rice, J. A., J. E. Breck, S. M. Bartell, and J. F. Kitchell. 1983. Evaluating the constraints of temperature, activity and consumption on growth of largemouth bass (*Micropterus salmoides*). Environmental Biology of Fishes 9: 263–276.

Simon, M. P. 1984. The influence of conspecifics on egg and larval mortality in amphibians. Pages 65–86 *in* G. Hausfater and S. B. Hrdy, eds. Infanticide: comparative and evolutionary perspectives. Aldine, New York.

Solomon, D. J., and A. E. Brafield. 1972. The energetics of feeding, metabolism and growth of perch (*Perca fluviatilis* L.). Journal of Animal Ecology 41:699–718.

Thorpe, J. E. 1977. Morphology, physiology, behavior, and ecology of *Perca fluviatilis* L. and *Perca flavescens* Mitchill. Journal of the Fisheries Research Board of Canada 34:1504–1514.

Treasurer, J. W. 1981. Some aspects of the reproductive biology of perch *Perca fluviatilis*: fecundity, maturation and spawning behavior. Journal of Fish Biology 18: 729–740

Tripet, F., and N. Perrin. 1994. Size-dependent predation by *Dugesia lugubris* (Turbellaria) on *Physa acuta* (Gastropoda): experiments and model. Functional Ecology 8:458–463

Van den Bosch, F., and W. Gabriel. 1997. Cannibalism in an age-structured predator-prey system. Bulletin of Mathematical Biology 59:551–567.

Van den Bosch, F., A. M. de Roos, and W. Gabriel. 1988. Cannibalism as a life boat mechanism. Journal of Mathematical Biology 26:619–633.

Van Densen, W. L. T. 1994. Predator enhancement in freshwater fish communities. Pages 102–119 *in* I. G. Cowx, ed. Rehabilitation of freshwater fisheries. Fishing News Books. Blackwell Scientific, Oxford.

Werner, E. E. 1988. Size, scaling and the evolution of life

cycles. Pages 60–81 *in* B. Ebenman and L. Persson, eds. Size-structured populations: ecology and evolution. Springer, Heidelberg.

Wilbur, H. M. 1988. Interactions between growing predators and growing prey. Pages 157–172 *in* B. Ebenman and L. Persson, eds. Size-structured populations: ecology and evolution. Springer, Heidelberg.

Willemsen, J. 1977. Population dynamics of percids in Lake IJssel and some smaller lakes in The Netherlands. Journal of the Fisheries Research Board of Canada 34: 1710–1719.

Associate Editor: Donald L. DeAngelis